J. Fluid Mech. (1991), *vol.* 223, *pp.* 25–45
Printed in Great Britain

Surface wave and thermocapillary instabilities in a liquid film flow

By D. A. GOUSSIS† AND R. E. KELLY

Mechanical, Aerospace, and Nuclear Engineering Department, University of California, Los Angeles, Los Angeles, CA 90024, USA

(Received 8 September 1988 and in revised form 28 February 1990)

A liquid film flowing down an inclined heated plane subject to surface wave and thermocapillary instabilities is studied. Three mechanisms exist by which energy can be transferred to the disturbance. Two of these mechanisms are associated with the thermocapillary forces and one with the shear stress of the basic flow at the deformed free surface. Depending on which mechanism is dominant, the instability can assume the form of either long transverse waves or short longitudinal rolls.

1. Introduction

An isothermal liquid layer flowing down an inclined plane might become unstable owing to surface or shear wave modes of instability. Except for very small angles of inclination, the surface wave mode causes instability first (Lin 1967; De Bruin 1974; Floryan, Davis & Kelly 1987). When a temperature gradient exists across the film, the flow might become unstable owing to thermocapillary or buoyancy forces as well. For moderate values of the Prandtl number Pr, the buoyancy mode causes instability first only when the angle of inclination is small (Kelly & Goussis 1982; Smith 1990*b*). On the other hand, the thermocapillary and surface wave modes compete in causing instability for all angles of inclination, at least for very long-wavelength disturbances (Kelly, Davis & Goussis 1986). Here, the surface wave and thermocapillary modes of instability will be considered for disturbances of finite wavelength, with the understanding that small angles of inclination are excluded.

The disturbance due to the surface wave mode originates at the free surface (hence surface wave instability) where vorticity is produced by the basic flow shear stress (Kelly *et al.* 1989; Smith 1990*a*). Owing to the effects of inertia, the perturbation vorticity tends to be advected downstream relative to the deflection of the free surface so as to cause instability. This shift is opposed by hydrodynamic and surface tension forces. Since the latter force is unimportant for large-wavelength disturbances, the instability manifests itself at these limiting values of wavelengths at the point where the effects of inertia balance the effects of hydrostatic forces. This balance is expressed by the relation

$$\frac{gH^3}{2\nu^2} = \frac{5\cos\beta}{4\sin^2\beta} \tag{1}$$

(Benjamin 1957; Yih 1963), where g is gravity, H is the depth of the film, ν is the kinematic viscosity, and β is the angle of inclination. Both the effects of inertia and the hydrostatic pressure force increase with the depth. If the depth of the layer is less

† Present address: Mechanical and Aerospace Engineering Department, Princeton University, Princeton, NJ 08544, USA.

than that indicated by (1), the hydrostatic pressure force dominates and the flow is stable. In the opposite case, the effects of inertia dominate and the flow is unstable. In the limit $\beta \to 90°$, (1) shows that $H \to 0$, i.e. the flow is unstable for all depths. Since the force which drives the disturbance points in the direction of the basic flow, the instability assumes the form of transverse waves which extract the maximum amount of energy (Yih 1955). In the following, this type of instability will be referred to as the hydrodynamic or H-mode.

When the liquid layer is horizontal and is bounded from below by a heated wall, instability might be caused by forces at a free surface which are due to surface tension variations produced by temperature gradients (Pearson 1958). There exist two distinct mechanisms by which thermal effects can lead to a destabilizing thermocapillary force. One mechanism (which in the following will be referred to as the P-mode) is associated with the interaction of the basic temperature with the perturbation velocity field. For the layer to be subject to this mode of instability, the following condition must be satisfied:

$$\left[-\frac{\mathrm{d}\sigma}{\mathrm{d}T}\Delta T\right]\frac{\rho c_p}{\mu h} > 32.073 \tag{2}$$

(Goussis & Kelly 1990), where σ is the surface tension, ΔT is the difference between the wall and the ambient temperatures, ρ is the density, c_p is the heat capacity, μ is the dynamic viscosity, and h is the heat transfer coefficient at the free surface. The physical aspects related to this mode all appear in the above necessary condition for instability. The product in the brackets is a measure of the thermocapillary forces, while ρc_p is a measure of the effects of convection in extracting energy from the basic state. Large values of these quantities are favourable for instability. The dynamic viscosity μ and the heat transfer coefficient h are measures of the energy loss due to viscous dissipation and of the heat loss through the free surface, respectively. For instability to occur, the energy transferred to the disturbance and the work done by the thermocapillary forces have to be enough to overcome both these kinds of losses. The mechanism for energy transfer is more effective when the depth of the liquid layer is large. As a result, when condition (2) is satisfied, sufficiently deep layers are unstable, while sufficiently shallow layers are stable (Goussis & Kelly 1990). Large-wavelength disturbances are stabilized via heat loss through the free surface, while short-wavelength disturbances are stabilized by viscous dissipation (Goussis 1986). Therefore, the critical wavelength is of the order of the layer's depth (Pearson 1958).

The other mechanism for the development of thermocapillary forces (in the following referred to as the S-mode) is associated with the modification of the basic temperature at the free surface by the surface deformation (Goussis & Kelly 1990). What mainly opposes the deformation is gravity. For disturbances of sufficiently short wavelength, surface tension also acts so as to suppress surface deformation. Therefore, instability with respect to this mode takes the form of large-wavelength disturbances for which the hydrodynamic pressure is the only stabilizing force. Instability occurs first when the balance between the thermocapillary forces and the forces due to the hydrodynamic forces turns in favour of the former. This balance is expressed by the relation

$$H^2\rho g = \frac{3}{2}\frac{\left[-\frac{\mathrm{d}\sigma}{\mathrm{d}T}\Delta T\right]}{\left[1+\frac{hH}{K}\right]} \tag{3}$$

(Smith 1966), where K is the coefficient of thermal conductivity. If the depth of the

layer is less than that indicated by the above equation, the layer is unstable. For both modes of thermocapillary instability the disturbance has no preferred direction.

For instability to occur owing to the H-mode a mean flow is necessary, while for instability to occur owing to the P- and S-modes a temperature difference across the film must be present. As a result, a single critical parameter (such as the Reynolds or Marangoni number) appropriate for all three modes of instability does not exist. However, from the discussion above of the different modes of instability, it seems that the depth of the film plays an important role in the different physical processes that compete for stability or instability in all three modes. At sufficiently thin layers, the hydrostatic pressure dominates the effects of inertia so that the flow is stable with respect to the H-mode. As the depth of the layer increases, inertia dominates and the flow becomes unstable. Similarly, when the layer is thin, the interaction of the basic temperature with the perturbation velocity cannot transfer enough energy to the disturbance, so that the layer is stable with respect to the P-mode. At sufficiently thick layers, such an energy transfer is possible and instability might occur. On the other hand, for thin layers the thermocapillary forces dominate the hydrostatic pressure forces and the layer is unstable with respect to the S-mode. As the layer thickens, the hydrostatic pressure force dominates and the layer becomes stable. Therefore, in the present analysis we shall consider as a critical parameter a non-dimensional number (the Archimedes number) which is a measure of the depth of the layer. In particular, a set of non-dimensional parameters will be used which is appropriate for a comparison of the theoretical results with experimental data (Kelly *et al.* 1986). In this set, the variation of each of the physical parameters which control the flow of a given fluid in the laboratory (i.e. the depth of the film, the angle of inclination, and the temperature difference across the film) appears in a single non-dimensional parameter only.

The results of several works, which are related to the problem examined here, provide some indication of how the surface wave and thermocapillary modes interact. When the angle of inclination is sufficiently large and the disturbance consists of long waves, the surface wave and thermocapillary instabilities reinforce each other (Lin 1975; Kelly *et al.* 1986). In particular, in the long-wavelength limit, the flow becomes unstable first with respect to transverse waves which extract the maximum amount of energy from the basic state (Kelly *et al.* 1986). This outcome of the interaction of the two instabilities does not hold for all wave forms. Sreenivasan & Lin (1978), considering small angles of inclination, show that the disturbance assumes the form of longitudinal rolls. In that case, the emergence of a preferred direction is entirely due to the presence of the shear flow. As in many other cases of thermoconvection (Gallagher & Mercer 1965; Gage & Reid 1968; Kelly & Goussis 1982), the shear flow tends to stabilize disturbances whose wavenumber vectors have a component in the streamwise direction, so that the instability at small angles assumes the form of longitudinal rolls. Clearly, for the present study to be complete, a disturbance of arbitrary orientation has to be considered.

2. The governing equations

In the derivation of the governing linear stability equations it is assumed that all physical properties, except the surface tension, are constant. In addition, the effects of compressibility and viscous dissipation are ignored. The surface tension is taken to depend on temperature in the form

$$\sigma = \sigma_0 + \left[\frac{\mathrm{d}\sigma}{\mathrm{d}T}\right]_0 (T - T_0), \tag{4}$$

where the subscript 0 refers to the free surface conditions. The dimensional velocity vector $\boldsymbol{u}$, temperature T, pressure P, and time τ, are scaled as

$$\boldsymbol{u} = U_r U^* \boldsymbol{i}_x + \frac{\nu}{H}\boldsymbol{u}', \quad U_r = \frac{gH^2 \sin\beta}{2\nu}, \tag{5}$$

$$T = \Delta T(T^* + \theta'), \quad \Delta T = (T_w - T_0), \tag{6}$$

$$P = \rho g H \cos\beta P^* + \rho \frac{\nu}{H} p', \tag{7}$$

$$\tau = \frac{H^2}{\nu} t \tag{8}$$

where U^*, T^*, and P^* are the non-dimensional basic flow velocity, temperature, and pressure respectively, the subscripts w and 0 refer to the conditions at the wall and at the ambient, respectively, and the primes denote perturbation quantities. In the following the primes and asterisks are dropped for convenience. With these scalings, the linearized non-dimensional stability equations (momentum and energy equations) for a three-dimensional disturbance become

$$u_t + \chi \sin\beta U u_x + \chi \sin\beta \mathrm{D}U w = -p_x + \nabla^2 u, \tag{9a}$$

$$v_t + \chi \sin\beta U v_x = -p_y + \nabla^2 v, \tag{9b}$$

$$w_t + \chi \sin\beta U w_x = -p_z + \nabla^2 w, \tag{9c}$$

$$\theta_t + \chi \sin\beta U \theta_x + w\mathrm{D}T = \frac{1}{Pr}\nabla^2\theta, \tag{9d}$$

where

$$\left.\begin{aligned} &\chi = \frac{gH^3}{2\nu^2}, \quad Pr = \frac{\nu}{\kappa}, \quad \nabla^2 = \frac{\partial^2}{\partial x^2} + \frac{\partial^2}{\partial y^2} + \frac{\partial^2}{\partial z^2}, \\ &U = 1 - z^2, \quad T = z - 1, \quad \mathrm{D} = \frac{\mathrm{d}}{\mathrm{d}z}, \end{aligned}\right\} \tag{10}$$

and the subscripts t, x, y, and z denote partial derivatives, and κ is the thermal diffusivity. The above equations are supplemented with the boundary conditions at the wall and the free surface. At the wall we have the no-slip, non-permeable, and isothermal conditions:

$$u = v = w = \theta = 0 \quad \text{at} \quad z = 1. \tag{11a–d}$$

At the free surface the normal and shear stress conditions, the heat balance, and the kinematic condition are

$$-2\chi \cos\beta \eta \mathrm{D}P - p + w_z + \frac{2\chi^{\frac{1}{3}}}{Bo}\nabla^2\eta = 0 \quad \text{at} \quad z = 0, \tag{12a}$$

$$\chi \sin\beta \mathrm{D}^2 U \eta + u_z + w_x = \frac{M}{Bi}\theta_{xz} \quad \text{at} \quad z = 0, \tag{12b}$$

$$v_z + w_y = \frac{M}{Bi}\theta_{yz} \quad \text{at} \quad z = 0, \tag{12c}$$

$$\theta_z = Bi\,\chi^{\frac{1}{3}}(\eta \mathrm{D}T + \theta) \quad \text{at} \quad z = 0, \tag{12d}$$

$$\eta_t + \chi \sin\beta U \eta_x = w \quad \text{at} \quad z = 0, \tag{12e}$$

where $$Bo = \frac{\rho}{\sigma}(4\nu^4 g)^{\frac{1}{3}}, \quad M = -\frac{\mathrm{d}\sigma}{\mathrm{d}T}\frac{\Delta T}{\rho\nu}\left(\frac{2}{\nu g}\right)^{\frac{1}{3}}, \quad Bi = \frac{h}{K}\left(\frac{2\nu^2}{g}\right)^{\frac{1}{3}}, \quad P = z, \tag{13}$$

and η is the non-dimensional free surface deflection. Substituting the following expressions for the perturbation quantities:

$$(w, \theta, \eta) = [F(z), \Theta(z), N]\exp[\mathrm{i}(k_x x + k_y y - \alpha t)], \tag{14}$$

where k_x and k_y are the real wavenumbers in the x- and y-directions, respectively, and α is the complex growth rate, the governing equations become

$$(\mathrm{D}^2 - k^2)^2 F + \mathrm{i}[(\alpha - k_x \chi \sin\beta U)(\mathrm{D}^2 - k^2) + k_x \chi \sin\beta \mathrm{D}^2 U]F = 0, \tag{15a}$$

$$(\mathrm{D}^2 - k^2)\Theta + \mathrm{i}Pr[(\alpha - k_x \chi \sin\beta U)\Theta + \mathrm{i}FDT] = 0, \tag{15b}$$

$$F(1) = \mathrm{D}F(1) = \Theta(1) = 0, \tag{15c–e}$$

$$(\mathrm{D}^3 - 3k^2\mathrm{D})F(0) + \mathrm{i}[\alpha - k_x \chi \sin\beta U(0)]\,\mathrm{D}F(0) + 2k^2\chi\left[\cos\beta + \frac{k^2}{Bo\chi^{\frac{2}{3}}}\right]N = 0, \tag{15f}$$

$$(\mathrm{D}^2 + k^2)F(0) - \mathrm{i}k_x \chi \sin\beta \mathrm{D}^2 U(0)\,N - k^2\frac{M}{Bi}\mathrm{D}\Theta(0) = 0, \tag{15g}$$

$$\mathrm{D}\Theta(0) = Bi\chi^{\frac{1}{3}}[N\mathrm{D}T(0) + \Theta(0)], \tag{15h}$$

$$N = \frac{\mathrm{i}F(0)}{\alpha - k_x \chi \sin\beta U(0)}, \tag{15i}$$

where $$k^2 = k_x^2 + k_y^2.$$

When $\beta = 0$, a mean flow does not exist and the instability is of thermocapillary origin with no preferred direction. When the plane is slightly tilted ($\beta \ll 1$), Sreenivasan & Lin (1978) show that the instability at $k = O(1)$ assumes the form of longitudinal rolls. In this case ($k_x = 0$), the basic velocity is absent from the governing equations. The marginal state is stationary (Takashima 1981; Goussis & Kelly 1990) and is described by the relation

$$2\chi\left(\frac{F_1}{M\chi^{\frac{1}{3}}} - PrF_2\right)\left(\cos\beta + \frac{k^2}{Bo\,\chi^{\frac{2}{3}}}\right) = F_3, \tag{16}$$

where $$F_1 = 8k(\sinh k\cosh k - k)(Bi\,\chi^{\frac{1}{3}}\sinh k + k\cosh k),$$

$$F_2 = \sinh^3 k - k^3\cosh k, \quad F_3 = 8k^5\cosh k$$

(Smith 1966; Sreenivasan & Lin 1978). In the $k \to 0$ limit (16) reduces to

$$\chi^{\frac{2}{3}} = \frac{3M}{4\cos\beta(1 + Bi\,\chi^{\frac{1}{3}})}. \tag{17}$$

Equation (17), apart from the term $\cos\beta$ which accounts for the component of gravity normal to the free surface, is identical to (3). In the limit $\beta \to 90°$, (17) shows that $\chi \to \infty$, i.e. the layer is unstable for all χ.

When the film is isothermal, the most unstable disturbance consists of transverse waves ($k_y = 0$). The situation is the same in the non-isothermal case, at least in the $k \to 0$ limit (Kelly *et al.* 1986). The equations governing the stability of the flow with

respect to this type of disturbance are obtained from (15a–i) by use of the transformations

$$F = ik\Phi, \quad \alpha = kc, \quad k = k_x, \tag{18}$$

where Φ is the normal mode amplitude of the stream function and c is the complex wavespeed. These equations are

$$(\mathrm{D}^2-k^2)^2\Phi + \mathrm{i}k[(c-\chi\sin\beta U)(\mathrm{D}^2-k^2)+\chi\sin\beta \mathrm{D}^2U]\,\Phi = 0, \tag{19a}$$

$$(\mathrm{D}^2-k^2)\,\Theta + \mathrm{i}k\,Pr[(c-\chi\sin\beta U)\,\Theta + \Phi \mathrm{D}T] = 0, \tag{19b}$$

$$\Phi(1) = \mathrm{D}\Phi(1) = \Theta(1) = 0, \tag{19c–e}$$

$$(\mathrm{D}^3-3k^2\mathrm{D})\,\Phi(0) + \mathrm{i}k[c-\chi\sin\beta U(0)]\,\mathrm{D}\Phi(0) + 2ik\chi\left[\cos\beta + \frac{k^2}{Bo\,\chi^{\frac{2}{3}}}\right]N = 0, \tag{19f}$$

$$(\mathrm{D}^2+k^2)\,\Phi(0) + \chi\sin\beta \mathrm{D}^2U(0)\,N - \mathrm{i}k\frac{M}{Bi}\mathrm{D}\Theta(0) = 0, \tag{19g}$$

$$\mathrm{D}\Theta(0) = Bi\,\chi^{\frac{1}{3}}[N\mathrm{D}T(0) + \Theta(0)], \tag{19h}$$

$$N = \frac{\Phi(0)}{c-\chi\sin\beta U(0)}. \tag{19i}$$

A small-wavenumber analysis yields the following relation for a neutral disturbance:

$$(\chi\sin\beta)^2 - \tfrac{5}{4}\chi\cos\beta + \frac{15}{16}\frac{M\chi^{\frac{1}{3}}}{1+Bi\,\chi^{\frac{1}{3}}} = 0. \tag{20}$$

The first and third terms represent the destabilizing effects of mean shear and thermocapillary forces, respectively, while the second term represents the stabilizing effects of gravity. When $M = 0$, the above relation reduces to (1) which defines the critical conditions for the surface wave mode of instability (H-mode). For longitudinal rolls, there is no mechanism to allow energy transfer from the mean flow to the disturbance, so that the term representing the mean shear is absent. In fact, if the first term in (20) is neglected one recovers (17), which defines the critical conditions for thermocapillary instability (S-mode) for large-wavelength disturbances. This result led to the conclusion that in the $k \to 0$ limit transverse waves are more unstable than longitudinal rolls (Kelly *et al.* 1986). In general, (20) yields two solutions for χ. One of these solutions corresponds to a surface wave instability (H-mode) as modified by the surface tension variation, while the other corresponds to a thermocapillary instability (S-mode) as modified by the shear flow. Equation (20) does not always admit a physically meaningful solution. For example, in the limit $\beta \to 90°$ there is no real and positive value of χ that can satisfy (20). Depending on the values of M and Bi, there is a value of β for which the two solutions of (20) coalesce. Beyond that value of β the flow is unstable for all χ, at least for large-wavelength disturbances. It can be shown that same situation occurs for a range of values of M and Bi.

It is seen that in the case of transverse wave both the surface wave and the thermocapillary modes can cause instability. In order to examine the relative importance of each of the two modes of instability, the equation for the rate of change of the kinetic energy of the disturbance will be examined. This equation in non-dimensional form is

$$\mathscr{K} + \mathscr{T} + \mathscr{H} = \mathscr{R} + \mathscr{S} + \mathscr{V} + \mathscr{D}, \tag{21}$$

where

$$\mathscr{K} = \frac{1}{2\lambda}\frac{\mathrm{d}}{\mathrm{d}t}\int_0^1\int_0^\lambda [u^2+w^2]\,\mathrm{d}x\,\mathrm{d}z, \tag{22a}$$

$$\mathscr{T} = \frac{2\chi^{\frac{1}{3}}}{Bo\,\lambda}\int_0^\lambda [-w\eta]_{z=0}\,\mathrm{d}x, \tag{22b}$$

$$\mathscr{H} = \frac{2\chi\cos\beta}{\lambda}\int_0^\lambda [w\eta]_{z=0}\,\mathrm{d}x, \tag{22c}$$

$$\mathscr{R} = \frac{\chi\sin\beta}{\lambda}\int_0^1\int_0^\lambda [-wu\mathrm{D}U]\,\mathrm{d}x\,\mathrm{d}y, \tag{22d}$$

$$\mathscr{S} = \frac{\chi\sin\beta}{\lambda}\int_0^\lambda [u\mathrm{D}^2U]_{z=0}\,\mathrm{d}x, \tag{22e}$$

$$\mathscr{V} = \frac{M}{Bi\,\lambda}\int_0^\lambda [-u\theta_{xz}]_{z=0}\,\mathrm{d}x, \tag{22f}$$

$$\mathscr{D} = -\frac{1}{\lambda}\int_0^1\int_0^\lambda [2(u_x)^2+(u_z+w_x)^2+2(w_z)^2]\,\mathrm{d}x\,\mathrm{d}z, \tag{22g}$$

where λ is the wavelength. When $M = 0$, (20) reduces to that developed for the isothermal problem (Kelly *et al.* 1989). The term $\mathscr{K}$ represents the time rate of change of the kinetic energy of the disturbance. The terms $\mathscr{T}$ and $\mathscr{H}$ represent the rate of work done against the surface tension and the hydrostatic pressure in deforming the free surface. These three terms are proportional to the growth rate kc_i and represent the way in which the total mean energy is distributed to the disturbance. The terms $\mathscr{R}$, $\mathscr{S}$, and $\mathscr{V}$, represent the rate of energy transfer to the disturbance by the Reynolds stress, by the shear stress of the basic flow at the free surface, and by the thermocapillary forces, respectively. $\mathscr{D}$ is always negative and denotes the rate at which energy is being dissipated by viscosity.

Solutions of the set of linear stability equations (15*a–i*) (or 19*a–i*) were obtained using the Tau method (Gottlieb & Orszag 1977), where the eigenfunction F (or Φ) and Θ were expanded in Chebyshev series. The Tau method resulted in a matrix eigenvalue problem of the form

$$(\boldsymbol{P}+\sigma\boldsymbol{Q}+\sigma^2\boldsymbol{R})\,\boldsymbol{X} = \boldsymbol{0}, \tag{23}$$

where σ is the eigenvalue (α or c), $\boldsymbol{P}$ is a fully populated matrix, $\boldsymbol{Q}$ has three rows of zeros (corresponding to the boundary conditions at the wall which do not involve the eigenvalue), and $\boldsymbol{R}$ has only rows of zeros except for one (corresponding to the normal stress condition which contains the eigenvalue in quadratic form). Using a transformation (Pearlstein & Goussis 1988), the above equation was put in the form

$$(\boldsymbol{S}+\sigma\boldsymbol{T})\,\boldsymbol{Y} = \boldsymbol{0}, \tag{24}$$

where the size of the system has increased by unity. The singularity of $\boldsymbol{Q}$ is preserved in $\boldsymbol{T}$ and produces three eigenvalues whose modulus is infinity. With another transformation (Goussis & Pearlstein 1989) these eigenvalues are mapped to prespecified points in the complex plane, while all finite eigenvalues are preserved. The eigenvalue problem thus formulated was solved by the QZ algorithm (Moler & Stewart 1973). Results thus obtained were compared with those existing in the literature for some limiting cases (Pearson 1958; Smith 1966) and with those

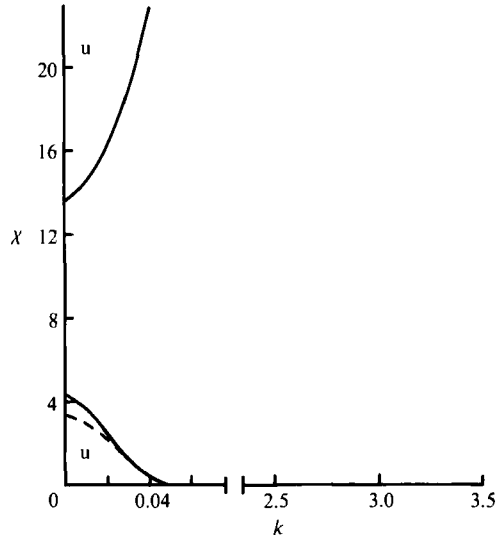

FIGURE 1. Neutral curves for $M = 45$, $Pr = 7$, $Bi = 10$, $Bo = 5 \times 10^{-4}$, $\beta = 15°$. ——, transverse waves; – – –, longitudinal rolls; u, unstable region.

obtained by the analytical solutions (16), (20). The agreement was excellent (Goussis 1986).

With the eigenvalue problem (19*a–i*) solved by representing the eigenfunctions F and Θ by Chebyshev series, the integrals in (21) were calculated by Simpson's one-third rule. Enough terms in the Chebyshev expansion were retained to assure that the residual in (21) was of the order of the error of the integration method.

3. Results and discussion

Figures 1–5 show neutral curves for transverse and longitudinal disturbances at different values of M. When M is sufficiently small, figure 1 shows that there exist two unstable regions in the (χ, k)-plane, both of which lie in the $k \ll 1$ region. The upper unstable region corresponds to the H-mode of instability as modified by the thermocapillary forces. The lower unstable region corresponds to the S-mode of instability as modified by the shear flow. For both cases the flow becomes unstable first with respect to transverse waves at $k_c = 0$. Therefore, the critical values $\chi_c = \chi_H$ and χ_S are given by the relation (20). As M increases, χ_H and χ_S approach each other. This is shown in figure 2, where it is also shown that another unstable region appears at $k = O(1)$. Instability there occurs when χ is sufficiently large, say $\chi > \chi_P$, and it assumes the form of longitudinal rolls. This unstable region is due to the P-mode and appears only when $MPr/Bi > 32.073$ (i.e. (2)). For the values of the parameters of figure 2, $\chi_H < \chi_P$ so that the flow is stable when $\chi_S < \chi < \chi_H$, as in the case of figure 1. With further increase of M, χ_H and χ_S still approach each each other while χ_P decreases. This is shown in figure 3, where now, since $\chi_P < \chi_H$, the flow is stable only when $\chi_S < \chi < \chi_P$. For a larger value of M, figure 4 shows that $\chi_P < \chi_S$ so that the flow is unstable for all values of χ. In addition, figure 4 shows that at $k = O(1)$ there is a closed region where the flow becomes unstable with respect to transverse waves as well. However, since this unstable region lies inside the region where the longitudinal rolls are unstable, it does not affect the stable region in the

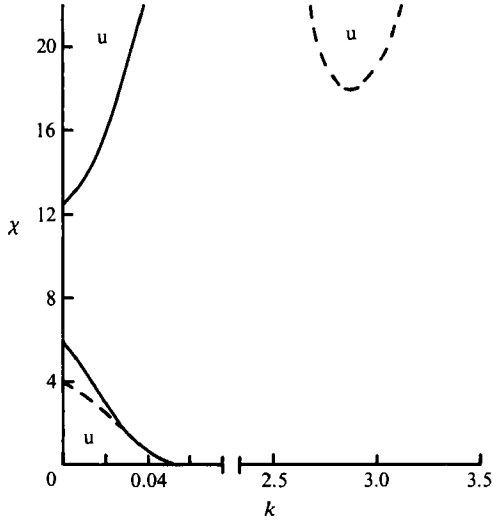

FIGURE 2. Neutral curves for $M = 51$, $Pr = 7$, $Bi = 10$, $Bo = 5 \times 10^{-4}$, $\beta = 15°$. ——, transverse waves; – – –, longitudinal rolls; u, unstable region.

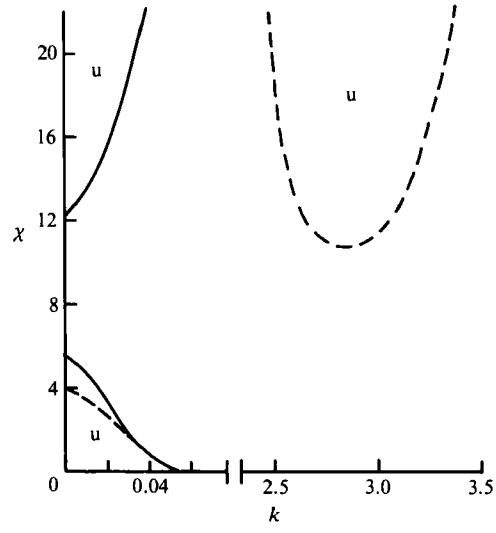

FIGURE 3. Neutral curves for $M = 52$, $Pr = 7$, $Bi = 10$, $Bo = 5 \times 10^{-4}$, $\beta = 15°$. ——, transverse waves; – – –, longitudinal rolls; u, unstable region.

(χ, k)-plane. There is a value of M, depending on Bi and β, such that $\chi_S = \chi_H$ (Kelly *et al.* 1986). Beyond this value of M the flow is unstable for all values of χ, at least for large-wavelength disturbances. Neutral curves for such a value of M are presented in figure 5, where it is shown that the two unstable regions in the $k \ll 1$ range unite, forming a single unstable region. For the values of the parameters in the sequence of figures 1–5, as M increases the flow becomes unstable for all values of χ first at the point where $\chi_S = \chi_P$. For different values of the parameters, the same situation can occur first at the point where $\chi_H = \chi_S$.

In order to examine the effects of the thermocapillary forces on the H-mode and the effects of the basic flow on the S- and P-modes, the terms in the rate of change

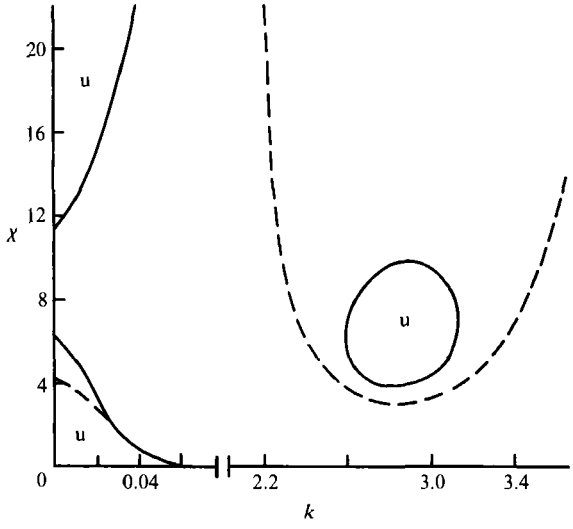

FIGURE 4. Neutral curves for $M = 55$, $Pr = 7$, $Bi = 10$, $Bo = 5 \times 10^{-4}$, $\beta = 15°$. ——, transverse waves; – – –, longitudinal rolls; u, unstable region.

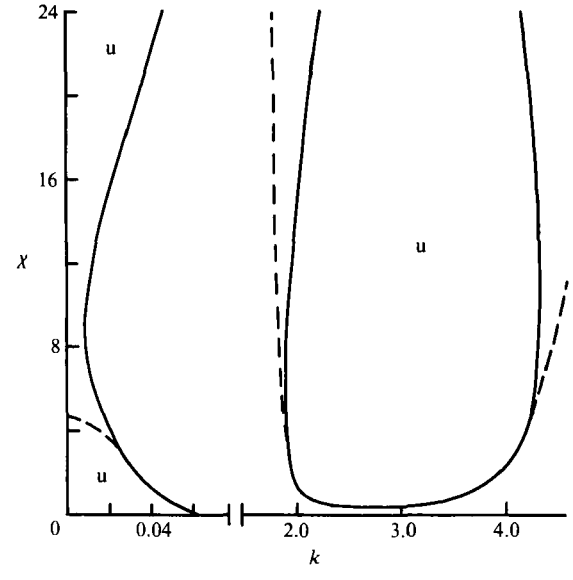

FIGURE 5. Neutral curves for $M = 65$, $Pr = 7$, $Bi = 10$, $Bo = 5 \times 10^{-4}$, $\beta = 15°$. ——, transverse waves; – – –, longitudinal rolls; u, unstable region.

of the kinetic energy equation for transverse waves (21) were evaluated for different values of χ and the parameters of figure 4. The physical meaning of the terms in (21) was explained previously: it is sufficient to say here that $\mathscr{V}$ is associated mainly with the S and P modes, while the term $\mathscr{S}$ is associated mainly with the H-mode. In the $k \ll 1$ region, table 1 shows that the terms $\mathscr{V}$ and $\mathscr{S}$ are positive for all values of χ, indicating that both the thermocapillary forces and the basic shear stress tend to cause instability. As expected, $\mathscr{V}$ decreases with increasing χ, while $\mathscr{S}$ increases. The term $\mathscr{R}$, although small, is positive. This indicates that some energy is transferred to the disturbance from the basic flow through the Reynolds stress. In the $k = O(1)$

	χ	c
1	0.1	$0.5175, 0.02136 \times 10^{-1}$
2	1	$0.5175, 0.01758 \times 10^{-1}$
3	10	$5.1764, -0.5252 \times 10^{-2}$
4	20	$10.3509, 0.03697 \times 10^{-1}$

	1	2	3	4
$\mathscr{K}$	0.7053×10^{-4}	0.5850×10^{-4}	-0.1747×10^{-4}	0.1232×10^{-3}
$\mathscr{T}$	0.8697×10^{-2}	0.2609×10^{-3}	-0.1685×10^{-5}	0.3746×10^{-5}
$\mathscr{H}$	0.9050×10^{-2}	0.1260×10^{-2}	-0.3778×10^{-4}	0.1333×10^{-3}
$\mathscr{R}$	0.6161×10^{-7}	0.6233×10^{-6}	0.3544×10^{-5}	0.2798×10^{-5}
$\mathscr{S}$	0.5874	0.9942	0.9997	1.0000
$\mathscr{V}$	0.4303	0.7363×10^{-2}	0.3992×10^{-3}	0.2303×10^{-3}
$\mathscr{D}$	−1.000	−1.000	−1.000	−1.000

TABLE 1. Values of the terms in the rate of change of kinetic energy equation (21) for different values of χ, $k = 0.01$, and the parameters of figure 4

	χ	c
1	2	$0.4528, -0.2508 \times 10^{-1}$
2	6	$1.3620, 0.8256 \times 10^{-2}$
3	12	$2.7446, -0.1132 \times 10^{-1}$
4	40	$9.3923, -0.2131$

	1	2	3	4
$\mathscr{K}$	-0.1520×10^{-2}	0.4989×10^{-3}	-0.6850×10^{-3}	-0.1288×10^{-1}
$\mathscr{T}$	-0.1172×10^{-2}	0.2907×10^{-3}	-0.3612×10^{-5}	-0.1396×10^{-5}
$\mathscr{H}$	-0.1069×10^{-10}	0.5513×10^{-11}	-0.1087×10^{-10}	-0.9392×10^{-9}
$\mathscr{R}$	-0.7974×10^{-5}	-0.7215×10^{-4}	-0.2999×10^{-3}	-0.3762×10^{-2}
$\mathscr{S}$	-0.1854×10^{-5}	-0.1164×10^{-5}	-0.3793×10^{-5}	-0.3058×10^{-4}
$\mathscr{V}$	0.9984	1.0005	0.9996	0.9907
$\mathscr{D}$	−1.000	−1.000	−1.000	−1.000

TABLE 2. Values of the terms in the rate of change of kinetic energy equation (21) for different values of χ, $k = 2.9$, and the parameters of figure 4

region, table 2 shows that the energy available for the disturbance to grow comes from the action of the thermocapillary forces only ($\mathscr{V} > 0$), while the basic shear stress at the free surface and the Reynolds stress in the bulk of the fluid tend to stabilize the flow ($\mathscr{S} < 0$ and $\mathscr{R} < 0$).

For the problem examined here, a Squire's transformation exists but Squire's theorem is not valid. This is demonstrated in figures 1–5, where it is shown that depending on the wavenumber, the flow becomes unstable first with respect to either transverse or longitudinal disturbances. As the results from the rate of change of kinetic energy equation show, this is entirely due to the effects of the basic flow on the action of the thermocapillary forces. Depending on the value of the wavenumber, the basic flow can either destabilize or stabilize the flow via the shear stress at the deformed free surface and the Reynolds stress in the bulk of the fluid. As noted earlier, these two mechanisms for energy transfer are absent when the axis of the disturbance lies in the direction of the flow (longitudinal rolls). In this case, this type of disturbance can be unstable only owing to the thermocapillary forces. As the axis

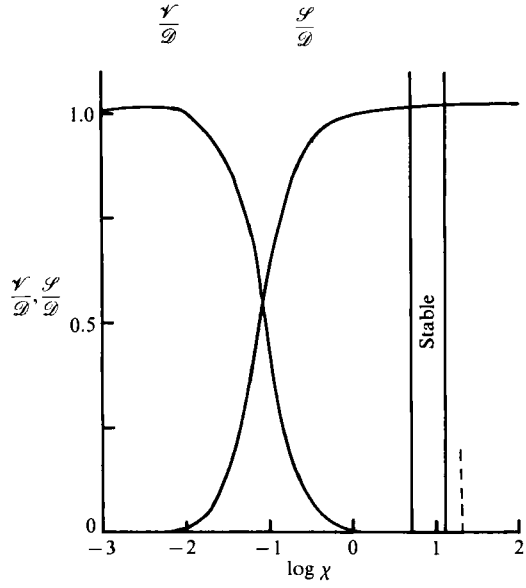

FIGURE 6. The variation of $\mathscr{V}/\mathscr{D}$ and $\mathscr{S}/\mathscr{D}$ for transverse waves, $k = 0.01$, and the parameters of figure 4.

of the disturbance is rotated, the effectiveness of the two hydrodynamic mechanisms for energy transfer increases, reaching a maximum when the axis lies perpendicular to the basic flow (transverse waves). As a result, in the $k \ll 1$ region where the basic flow and the thermocapillary forces reinforce each other, the most unstable disturbance consists of transverse waves. On the other hand, in the $k = O(1)$ region, where the basic flow opposes the action of the thermocapillary forces, the most unstable disturbance consists of longitudinal rolls.

In order to determine how the H- and S-modes reinforce each other in causing instability in the $k \ll 1$ region, the terms $\mathscr{V}$ and $\mathscr{S}$ of (21) were plotted against χ for fixed k. The results for the parameters of table 1 are shown in figure 6. When $M = 0$, the flow is unstable beyond the value of χ, denoted by the broken line, due to the H-mode. However, when $M \neq 0$, the flow becomes unstable at small values of χ as well and the stable region is reduced as shown in the figure. When $\chi \ll 1$, figure 6 shows that $\mathscr{V} = O(1)$ and $\mathscr{S}$ is negligible, indicating that the instability there is due to the S-mode. As χ increases, $\mathscr{V}$ decreases, while $\mathscr{S}$ increases. Even before χ reaches the lower neutral curve, $\mathscr{V}$ becomes negligible and $\mathscr{S} = O(1)$, indicating that the instability there is due to the H-mode. However, since the instability at small values of χ occurs only when $M \neq 0$, it is clear that the small contribution from the S-mode is essential. The same is true for the region beyond the upper neutral curve. The small influence of the S-mode there is sufficient to lower significantly the value of χ for neutral stability.

In the $k = O(1)$ region where the flow becomes unstable owing to the P-mode, the basic flow has a stabilizing effect on this mode of instability so that the disturbance assumes the form of longitudinal rolls. This stabilizing influence is exercised by the Reynolds stress inside the layer and by the basic shear stress at the deformed free surface. In order to examine the relative importance of these two stabilizing mechanisms of the basic flow in the case of transverse waves, the variation of the ratio $\mathscr{R}/\mathscr{S}$ as a function of χ was examined for the parameters of table 2. The results

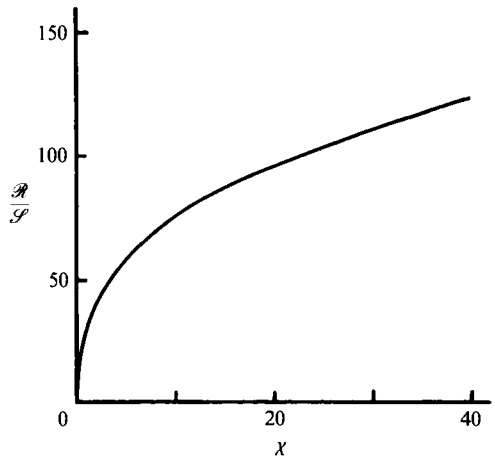

FIGURE 7. The variation of $\mathscr{R}/\mathscr{S}$ for transverse waves, $k = 2.90$, and the parameters of figure 4.

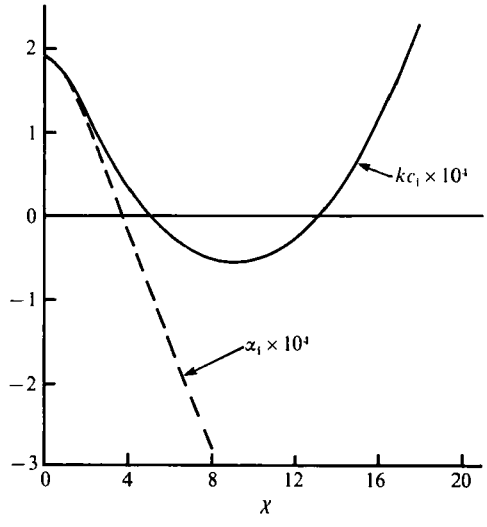

FIGURE 8. The variation of the growth rate with χ for transverse (——) and longitudinal (– – –) disturbances for $k = 0.01$ and the parameters of figure 4.

are presented in figure 7 where it is shown that, except in the $\chi \ll 1$ region, the effect of the Reynolds stress is larger than the effect of the basic shear stress at the free surface. In the $k = O(1)$ region, $c < \chi \sin\beta$ so that a critical layer is developed (Goussis 1986). In other cases (i.e. Tollmien–Schlichting waves), the emergence of a critical layer can be accompanied by energy transfer to the disturbance through the Reynolds stress. However, as the results of table 2 show, the appearance here of a critical layer allows the basic flow to have a stabilizing influence.

The growth rates of the different types of disturbances reflect the outcome of the interaction of the surface wave and thermocapillary instabilities discussed above. In the $k \ll 1$ region where the H- and S-modes reinforce each other, figure 8 shows that the growth rate of transverse waves is always larger than that of longitudinal rolls. On the other hand, in the $k = O(1)$ region, where the basic flow has a stabilizing influence, figure 9 shows that the opposite is true. In addition, these figures show that

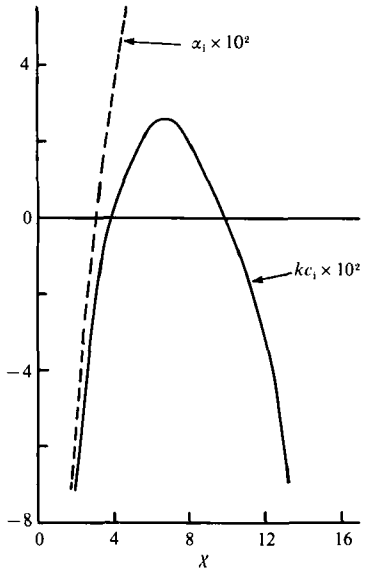

FIGURE 9. The variation of the growth rate with χ for transverse (——) and longitudinal (– – –) disturbances for $k = 2.90$ and the parameters of figure 4.

the instability due to the H- and S-modes (figure 8) yields a smaller growth rate than the instability due to the P-mode (figure 9). Apparently, the mechanism for energy transfer to the disturbance for the P-mode of instability is more efficient than the mechanism for the H- and S-modes.

For all practical considerations, the value of the Bond number Bo is very small. As figures 1–5 show, in this case the unstable regions due to the H- and S-modes (for which the surface deformation is essential) are restricted to the $k \ll 1$ region. For χ fixed, the effects of surface tension in suppressing the surface deformation increase as k increases. However, at the same time the effects of thermal convection inside the layer in producing a larger temperature variation along the free surface increase as well (Goussis & Kelly 1990). If Bo is sufficiently small, the restoring force due to surface tension stabilizes both the H- and S-modes before the effects of convection become important. As a result, the instability with respect to these modes occurs at $k_c = 0$. When $k = O(1)$ and $Bo \ll 1$, the normal stress condition (19f) shows that the free surface can be considered as non-deformable. Therefore, in the $k = O(1)$ region the H- and S-modes are absent and instability can occur due to the P-mode only.

In the unlikely case where Bo becomes large, the picture described above changes. This is shown in figure 10, where neutral curves are presented for the parameters of figure 2 except Bo, which now attains relatively large values. Figure 10 shows that as Bo increases, the instability at $k = O(1)$ occurs at a smaller value of χ. This is due to the fact that the effects of surface deformation now become important. Therefore, the temperature variation at the free surface produced by the P-mode is augmented by the modified basic temperature there, resulting in larger thermocapillary forces. In addition, figure 10 shows that the neutral curves which originate from the $k = 0$ axis are now extended further inside the (χ, k)-plane where the effects of convection are important. The result is that the P-mode reinforces the H- and S-modes so that the instability which occurs in the $k \ll 1$ region now initiates at $k_c \neq 0$. The overall effects of increasing Bo is to decrease the range of values of χ for which the flow is

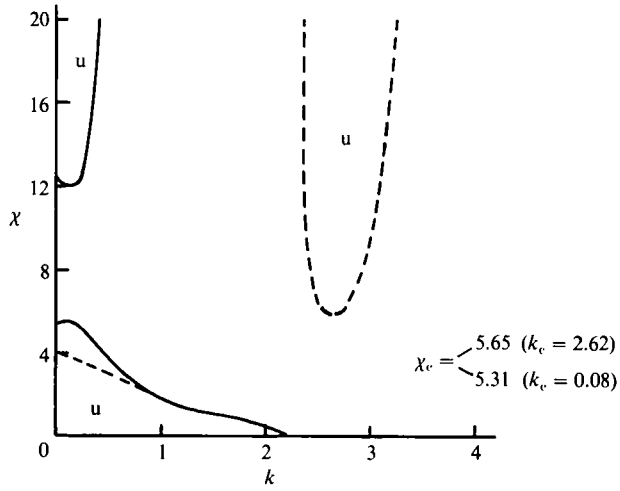

FIGURE 10. Neutral curves for $M = 51$, $Pr = 7$, $Bi = 10$, $Bo = 0.30$, $\beta = 15°$. ——, transverse waves; – – –, longitudinal rolls; u, unstable region.

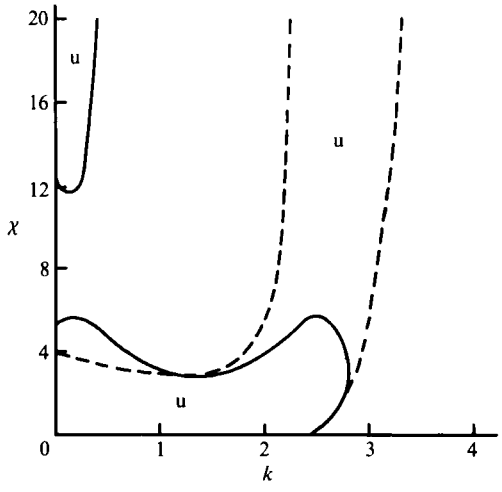

FIGURE 11. Neutral curves for $M = 51$, $Pr = 7$, $Bi = 10$, $Bo = 0.50$, $\beta = 15°$. ——, transverse waves; – – –, longitudinal rolls; u, unstable region.

stable. For even larger Bo, figure 11 shows that the unstable regions due to the S- and P-modes unite, thus making the flow unstable for all values of χ. The variation of χ_c with Bo is presented in figure 12, where it is shown that the stability boundaries are independent of Bo for all realistic values of this parameter.

The neutral curves presented in figure 1–5 show that the range of values of χ for which the flow is stable decreases as M increases. The variation of χ_c with M is presented in figure 13. For the values of χ for which the flow is stable when $M = 0$, the instability that occurs with increasing M assumes the form of transverse waves when χ is sufficiently small or large, while for intermediate values of χ the instability assumes the form of longitudinal rolls. As the sequence of figures 1–5 shows, as M increases the flow becomes unstable first with respect to longitudinal rolls only when $\chi_S < \chi_P < \chi_H$. However, if the two unstable regions in the $k \ll 1$ range unite before

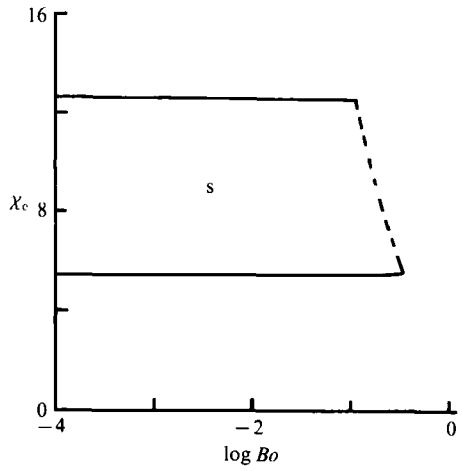

FIGURE 12. The variation of χ_c with Bo for $M = 51$, $Pr = 7$, $Bi = 10$, $\beta = 15°$. ——, transverse waves; – – –, longitudinal rolls; s, stable region.

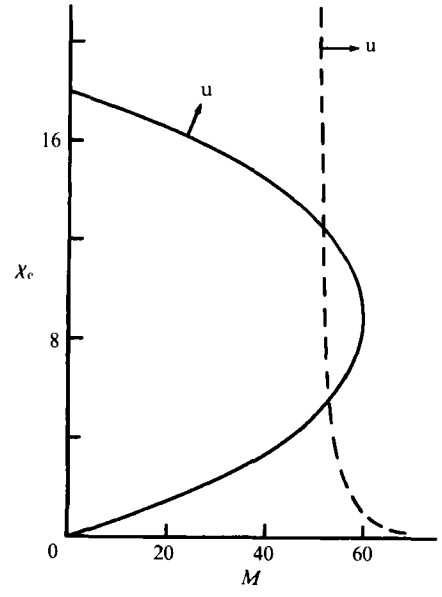

FIGURE 13. The variation of χ_c with M for $Pr = 7$, $Bi = 10$, $Bo = 5 \times 10^{-4}$, $\beta = 15°$. ——, transverse waves; – – –, longitudinal rolls; u, unstable region.

$\chi_P < \chi_H$, the flow becomes unstable first with respect to transverse waves for all values of χ. Such a case is presented in figure 14 for the parameters of figure 12, except Bi which is now smaller. It is shown that the stable region decreases with decreasing Bi and that longitudinal rolls are not accounted for in the stability boundaries.

When Bo is sufficiently small, the effects of surface deformation on the P-mode are negligible. As a result, this mode is independent of β. The H- and S-modes depend strongly upon β. Noting that $\chi \cos\beta$ is a measure of the hydrostatic pressure (which stabilizes the H- and S-modes) and $\chi \sin\beta$ is a measure of the inertia of the basic flow

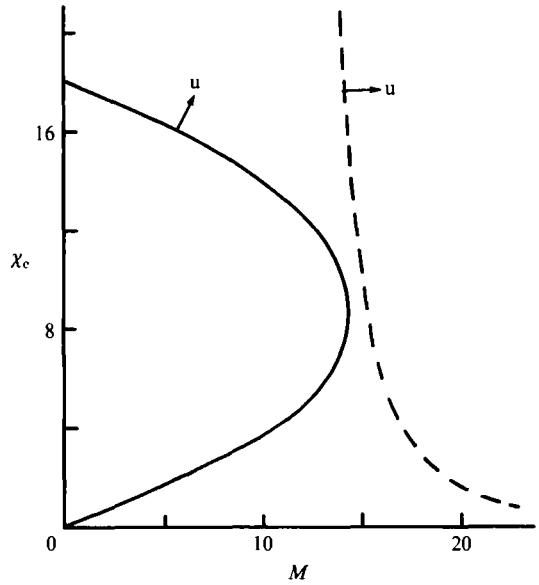

FIGURE 14. The variation of χ_c with M for $Pr = 7$, $Bi = 2$, $Bo = 5 \times 10^{-4}$, $\beta = 15°$. ——, transverse waves; – – –, longitudinal rolls; u, unstable region.

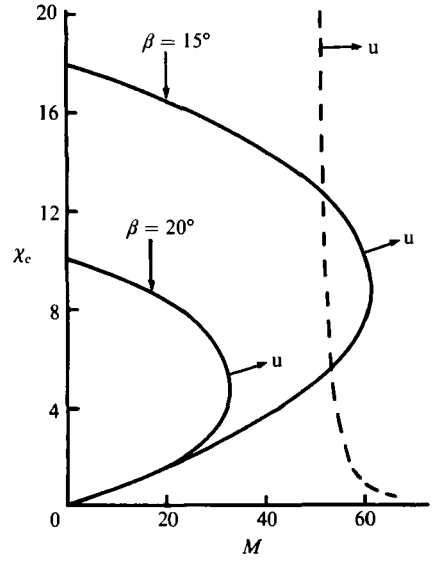

FIGURE 15. The variation of χ_c with M for two values of β, $Pr = 7$, $Bi = 10$, $Bo = 5 \times 10^{-4}$. ——, transverse waves; – – –, longitudinal rolls; u, unstable region.

(which is essential for the H-mode), this dependence is clear. Figure 15 shows the variation of χ_c with M for two values of β. For fixed χ, increasing β reduces the effects of the restoring force due to the hydrostatic pressure and increases the effects of the inertia of the basic flow, thus destabilizing the flow with respect to the H- and S-modes. Since $Bo \ll 1$, the variation of β does not change the stability boundaries due to the P-mode. In addition, figure 15 suggests that there is a value of β beyond which longitudinal rolls are not important in determining the stability boundaries.

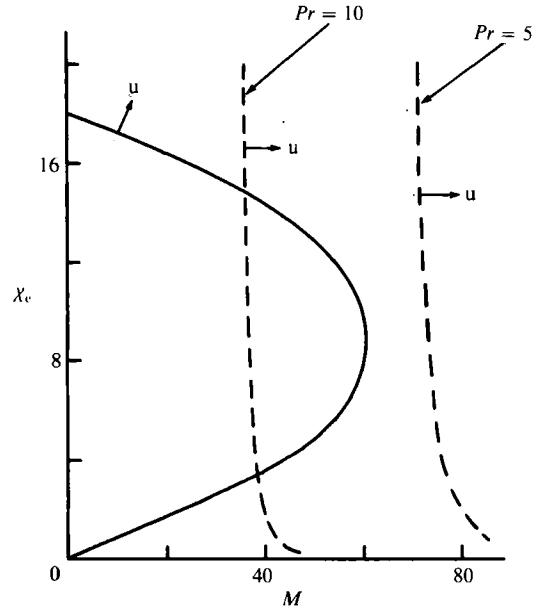

FIGURE 16. The variation of χ_c with M for two values of Pr, $Bi = 10$, $Bo = 5 \times 10^{-4}$, $\beta = 15°$. ——, transverse waves; – – –, longitudinal rolls; u, unstable region.

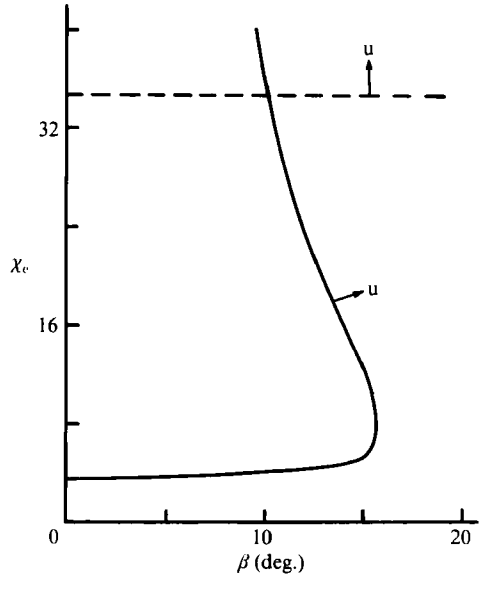

FIGURE 17. The variation of χ_c with β for $M = 50$, $Pr = 7$, $Bi = 10$, $Bo = 5 \times 10^{-4}$. ——, transverse waves; – – –, longitudinal rolls; u, unstable region.

Figure 16 shows the variation of χ_c with M for two values of Pr. When Bo is sufficiently small, $k_c = 0$ for the H- and S-modes. The effects of convection are absent there, so the corresponding χ_c is independent of Pr. However, the manifestation of the P-mode, for which the effects of convection are important, depends strongly upon

Pr. As figure 16 shows, decreasing values of Pr stabilize the P-mode, while the H- and S-modes remain unaffected. Therefore, the stable region initially increases as Pr decreases. However, as figure 16 suggests, there is a value of Pr below which the stability boundaries do not change.

For the problem considered here, the results of an experiment for a given liquid can be controlled by changing either χ (i.e. the flow rate), M (i.e. the temperature difference across the film), or β. The variation of χ_c with β is presented in figure 17. When $\beta = 0$, the layer becomes unstable owing to the S- and P-modes (the latter only when $MPr/Bi > 32.073$) for sufficiently small and large values of χ, respectively. As β increases from zero, a mean flow is generated which can cause instability due to the H-mode. Increasing values of β denote higher effects of the inertia of the basic flow and lower effects of the hydrostatic pressure. Therefore, the value of χ_c corresponding to the H-mode decreases as β increases. However, the value of χ_c associated with the S-mode increases with increasing β. This is because the hydrostatic pressure decreases and in addition the effects of main shear in reinforcing the S-mode increase. If $Bo \ll 1$, the P-mode is unaffected by the change of β so that the associated χ_c remains constant. The result is that with increasing β, the range of values of χ for which the flow is stable decreases.

4. Conclusions

The occurrence of thermocapillary and surface wave instabilities in a film flow has been examined. There exist three different mechanisms by which energy is transferred to the disturbance. For two of these mechanisms the deformation of the free surface is essential. Surface deformation modifies the basic temperature there (thus allowing the development of thermocapillary forces) and at the same time produces a non-zero shear stress due to the basic flow (thus generating an opposing disturbance shear stress). The resulting two modes of instability occur either when the film is thin and the liquid is relatively viscous or when the film is thick and the liquid is less viscous, respectively. While the thermocapillary modes gives no preferred direction, the hydrodynamic mode extracts the maximum amount of energy when the disturbance consists of transverse waves. Since the two modes reinforce each other, the disturbance for both types of instability takes the form of such waves. Both the hydrostatic pressure and the surface tension stabilize the two modes. Since the latter force is effective at relatively short-wavelength disturbances, the instability due to both modes takes the form of long waves.

The third mechanism is also associated with the thermocapillary forces at the free surface. In this case, the development of these forces is a result of the interaction of the basic temperature gradient with the perturbation velocity. Since, the effects of convection are important, instability occurs at short wavelengths. At large and very short wavelengths the heat loss through the surface and the dissipation in the film, respectively, prevail so that the flow is more stable. For this mode, the basic flow stabilizes the disturbances whose wavenumber vectors have a component in the streamwise direction, so that the disturbance assumes the form of longitudinal rolls. This type of instability exists only when condition (2) is satisfied and occurs at sufficiently thick layers and large temperature gradients.

Depending on which of these three mechanisms is the dominant one, the instability will first assume the form of either transverse waves or longitudinal rolls. When condition (2) is not satisfied, the instability will always take the form of transverse

waves. In that case and for realistic values of Bo, the critical conditions are determined by (20). Similar results arise when condition (2) is satisfied but $\chi_P > \chi_H$. That happens when Pr and Bi are sufficiently small or when β is sufficiently large. In the case where the flow is unstable with respect to both transverse waves and longitudinal rolls, the disturbance will presumably assume the latter form, which exhibits the largest growth rate.

The support of NSF under Grant No. 82-0944 is gratefully acknowledged.

REFERENCES

BENJAMIN, T. B. 1957 Wave formation in laminar flow down an inclined plane. *J. Fluid Mech.* **2**, 554.

DE BRUIN, G. J. 1974 Stability of a layer of liquid flowing down an inclined plane. *J. Engng Maths* **8**, 259.

FLORYAN, J. M., DAVIS, S. H. & KELLY, R. E. 1987 Instabilities of a liquid film flowing down a slightly inclined plane. *Phys. Fluids* **30**, 983.

GAGE, K. S. & REID, W. H. 1968 The stability of thermally stratified plane Poiseuille flow. *J. Fluid Mech.* **33**, 21.

GALLAGHER, A. P. & MERCER, A. 1965 On the behavior of small disturbances in plane Couette flow with a temperature gradient. *Proc. R. Soc. Lond.* A **286**, 117.

GOTTLIEB, D. & ORSZAG, S. A. 1977 *Numerical Analysis of Spectral Methods: Theory and Applications.* Philadelphia: SIAM.

GOUSSIS, D. A. 1986 Instabilities of stratified film flows. Ph.D. thesis, University of California, Los Angeles.

GOUSSIS, D. A. & KELLY, R. E. 1990 On the thermocapillary instabilities in a liquid layer heated from below. *Intl J. of Heat Mass Transfer* (in press).

GOUSSIS, D. A. & PEARLSTEIN, A. J. 1989 Removal of infinite eigenvalues in the generalized eigenvalue problem. *J. Comput. Phys.* **84**, 242.

KELLY, R. E., DAVIS, S. H. & GOUSSIS, D. A. 1986 On the instability of heated film flow with variable surface tension. In *Heat Transfer 1986.* Proc. 9th Intl Heat Transfer Conference, San Francisco, vol. 4, p. 1936.

KELLY, R. E. & GOUSSIS, D. A. 1982 Instability of a liquid film flowing down a heated inclined plane. In *Heat Transfer 1982.* Proc. 8th Intl Heat Transfer Conference, Munich, vol. 5, p. 319.

KELLY, R. E., GOUSSIS, D. A., LIN, S. P. & HSU, F. K. 1989 The mechanism for surface wave instability in liquid film flow. *Phys. Fluids* A **1**, 819.

LIN, S. P. 1967 Instability of a liquid film flowing down an inclined plane. *Phys. Fluids* **10**, 308.

LIN, S. P. 1975 Stability of liquid flow down a heated inclined plane. *Lett. Heat Mass Transfer* **2**, 361.

MOLER, G. B. & STEWART, G. W. 1973 An algorithm for the generalized eigenvalue problem. *SIAM J. Numer. Anal.* **10**, 241.

PEARLSTEIN, A. J. & GOUSSIS, D. A. 1988 Efficient transformation of singular polynomial matrix eigenvalue problems. *J. Comput. Phys.* **78**, 305.

PEARSON, J. R. A. 1958 On convection cells induced by surface tension. *J. Fluid Mech.* **4**, 489.

SMITH, K. A. 1966 On convective instability induced by surface tension gradients. *J. Fluid Mech.* **24**, 401.

SMITH, M. K. 1990*a* The mechanism for the long-wave instability in thin liquid films. *J. Fluid Mech.* **217**, 469.

SMITH, M. K. 1990*b* The long-wave instability in heated or cooled inclined liquid layers. *J. Fluid Mech.* **219**, 337.

SREENIVASAN, S. & LIN, S. P. 1978 Surface tension driven instability of a liquid film down a heated incline. *Intl J. Heat Mass Transfer* **21**, 1517.

TAKASHIMA, M. 1981 Surface tension driven instability in a liquid layer with a deformable free surface. *J. Phys. Soc. Japan* **50**, 2745.

YIH, C.-S. 1955 Stability of laminar parallel flow with a free surface. In *Proc. 2nd US Natl Congr. Applied Mechanics*, p. 623. ASME.

YIH, C.-S. 1963 Stability of liquid flow down an inclined plane. *Phys. Fluids* **6**, 321.